The X-Ray Activity of Sgr A*: Constraints on the Flaring-Source Size and Radial Distance from Sgr A* During the 2011 XMM-Newton Campaign

Enmanuelle Mossoux [1], Nicolas Grosso [1], Frédéric H. Vincent [2], Delphine Porquet [1]

[1] Observatoire Astronomique de Strasbourg, Université de Strasbourg, CNRS, UMR 7550, Strasbourg, France; [2] Nicolaus Copernicus Astronomical Center, Warszawa, Poland.

Introduction

Sgr A* is the closest supermassive black hole ($\approx 4 \times 10^6\ M_\odot$) located at the dynamical center of our galaxy. It has a very low bolometric luminosity ($\approx 10^{36}$ erg s^{-1}) and, consequently, a very low mass accretion rate ($\approx 10^{-6}\ M_\odot$/yr) but flaring activity can be observed in near-infrared, X-rays, sub-millimeter and radio. To constrain the origin of such activity, it is important to investigate the timing and spectral properties of these flares, especially in X-rays.

X-ray observations of Sgr A* were obtained with XMM-Newton on 2011 March 28 and 30 and April 1, 3, and 5 (AO-8, 5×33 ks; PI: D. Porquet) in coordination with VLBI observations at 1.3 mm (PI: S. Doeleman).

The results of this XMM-Newton campaign are published in Mossoux, E., Grosso, N., Vincent, F. H. & Porquet, D. (2015, A&A, 573, A46).

Timing analysis of Sgr A*

Extraction regions:

- For Sgr A* (*src+bkg* region): circle with a radius of 10″ centered on its radio coordinates.
- For the instrumental (flaring) background (*bkg* region): large square in the same CCD where resolved sources are removed.

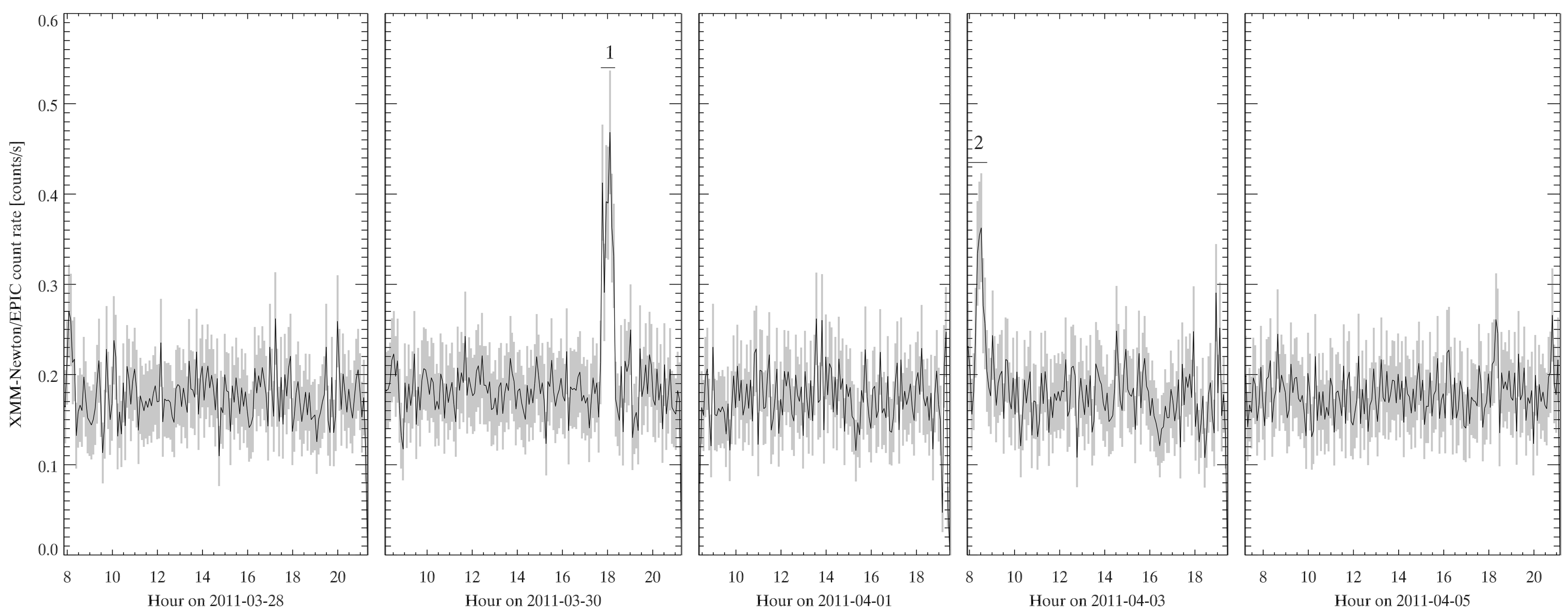

Figure 1: XMM-Newton (pn+MOS1+MOS2) light curve from 2 to 10 keV with a bin time of 300s. The two flares detected with the Bayesian-blocks method are labeled "1" and "2". The horizontal lines below these labels indicate the flare durations.

X-ray flare detection

The Bayesian-blocks analysis:

- Recursive algorithm working on the X-ray arrival times to find the times at which the count rate is statistically different (Scargle et al., 1998, ApJ, 504, 405; Scargle et al., 2013a, ApJ, 764, 167).
- We calibrate the prior vs. the number of events and the false detection probability 3%.
- We correct of the instrumental background with a two-step algorithm: searching the blocks (dashed lines in Fig. 2) on the *src+bkg* region and then on the *bkg* region and computing the weight of each photons (Scargle et al., 2013b, ArXiv:1304.2818). We can then compute the Bayesian-blocks of the *src* region by applying the weight on the photons from the *src+bkg* region.

The smoothed light curve:

- We use a density estimator on the X-ray arrival times using an Epanechnikov smoothing kernel with a window width of 100 s.
- We apply the weight computed from our two-step algorithm to produce directly the smoothed light curve corrected from the instrumental background.

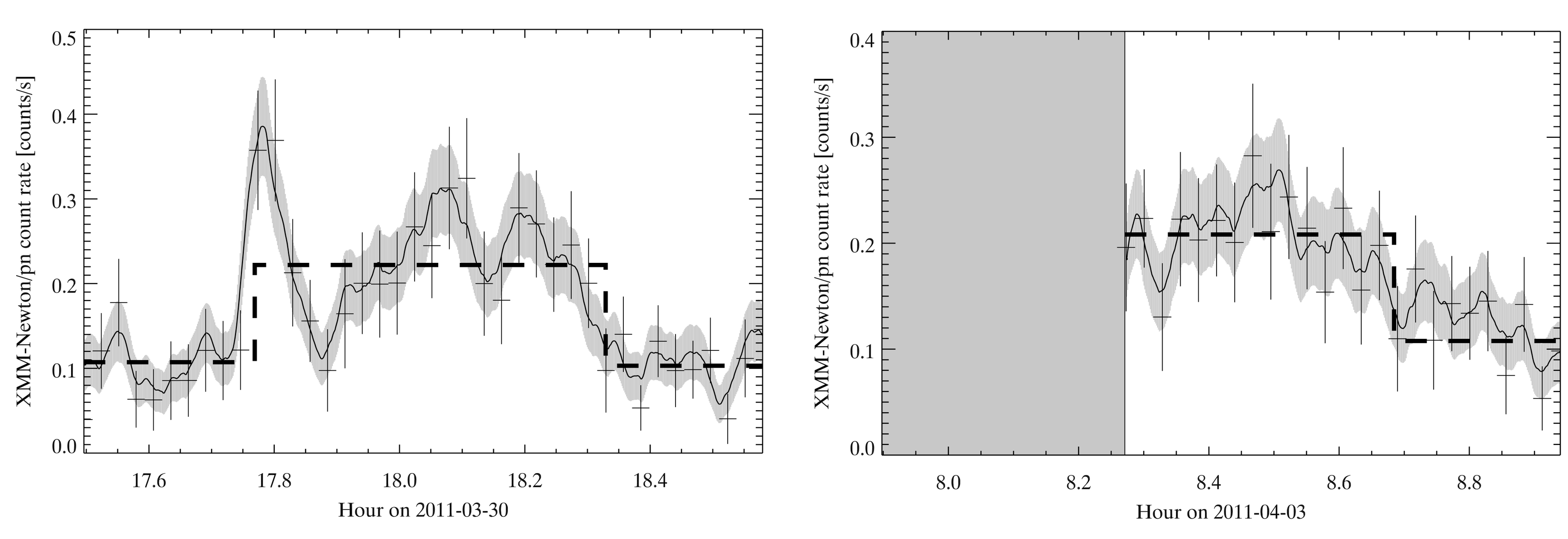

Figure 2: The pn light curve binned on 100s of the March 30 (left panel) and April 3 (right panel), 2011 flares. The dashed line shows the Bayesian blocks and the solid line is the smoothed light curve with the gray error bar.

A hotspot model for the 2011 March 30 flare

- The light curve of an hotspot orbiting has a double-bump shape: the short bump is due to the gravitational lensing when the black hole is located between the observer and the hotspot. The larger bump is due to the relativistic beaming effect when the hotspot is moving towards the observer.
- The first X-ray flare observed on March 30, 2011 is characterized by two sub-flares: the first one is very short ($\approx$ 458 s), whereas the second one is longer ($\approx$ 542 s) with a lower unabsorbed peak-luminosity. The waiting time between the two sub-flares ($\approx$ 1000 s) is one of the smallest ever observed.

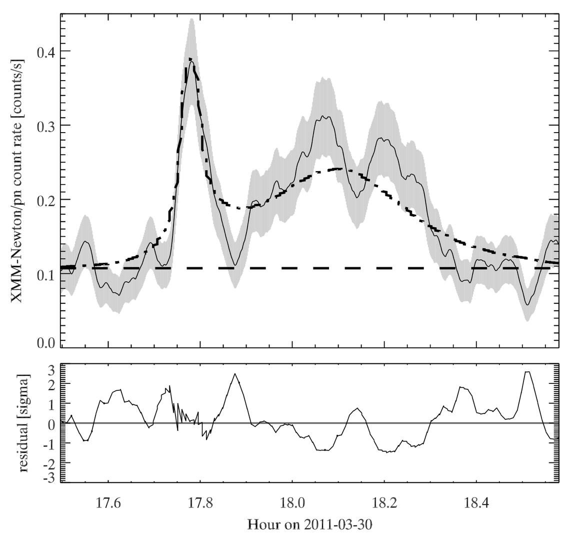

Figure 3: Best-fit light curve (dot-dashed line) of the pn March 30, 2011 flare. The non-flaring level is the dashed line. Lower panel: the residual in units of σ.

- The hotspot is a sphere of radius R, optically thin and in solid rotation with inclination i around Sgr A* (spin $a = 0.99$) at orbital radius r with Keplerian motion. The emitted spectrum is a powerlaw.
- We use the ray-tracing code GYOTO (Vincent et al., 2011, Class. Quant. Grav., 28, 5011) to make a χ^2-fitting on the smoothed pn light curve for 3 physical parameters: $r/r_{\rm g} \in [10.5, 12.5]$ by step of 0.5, $R/r_{\rm g} \in [1.2, 2.2]$ by step of 0.2, $i \in [81.93°, 87.66°]$ by step of 1.15°.

$\Rightarrow$ The best-fit parameters are $r = 12r_{\rm g}$, $R = 1.4r_{\rm g}$, $i = 86.5°$ with $\chi^2_{\rm red} = 0.85$, but we cannot satisfactorily reproduce the large decay of the light curve between the two sub-flares with this model.

Constraining the flaring-source properties

Magnetic energy heating during the flare-rise phase:

- We convert the observed rise and decay durations of the flare to proper-time durations $\Delta\tau(r)$ at a radial distance r from Sgr A*.
- The energy released during the entire first 2011 March 30 sub-flare is powered by the magnetic energy $U_{\rm B}$ available inside the flaring region of radius $R < c\Delta\tau_{rise}(r)$.
- The magnetic field B is $\propto r^{-1}$ with $B = 100$ G at $2\,r_{\rm g} = 0.08$ AU.
- The X-ray photons production efficiency for an unabsorbed flare luminosity $L^{\rm unabs}_{2-10\ {\rm keV}}({\rm flare})$ is $\eta = L^{\rm unabs}_{2-10\ {\rm keV}}({\rm flare})\Delta\tau_{\rm flare}/U_{\rm B}$.

  $\Rightarrow r < 100^{+19}_{-29}\ r_{\rm g}$ and $R < 2.87 \pm 0.01\ r_{\rm g}$ (left panel of Fig. 4).

Synchrotron cooling during the decay phase:

- The X-ray photons cool too rapidly to be the primary source of synchrotron cooling $\Rightarrow \tau_{\rm decay}$ due to the synchrotron cooling of accelerated electrons producing NIR photons. The X-ray photons are produced by the NIR photons via the Inverse Compton or Synchrotron Self-Compton process.
- The synchrotron cooling timescale (solid line) $\tau_{\rm sync} = 8 \times (B/30\ {\rm G})^{-3/2} \times (\nu/10^{14}\ {\rm Hz})^{-1/2}$ min (Dodds-Eden et al., 2009, ApJ, 698, 676) must be larger than $\Delta\tau_{\rm decay}$.

  $\Rightarrow 4\ r_{\rm g} < r$ (vertical lines) and $1.8\ r_{\rm g} < R$.

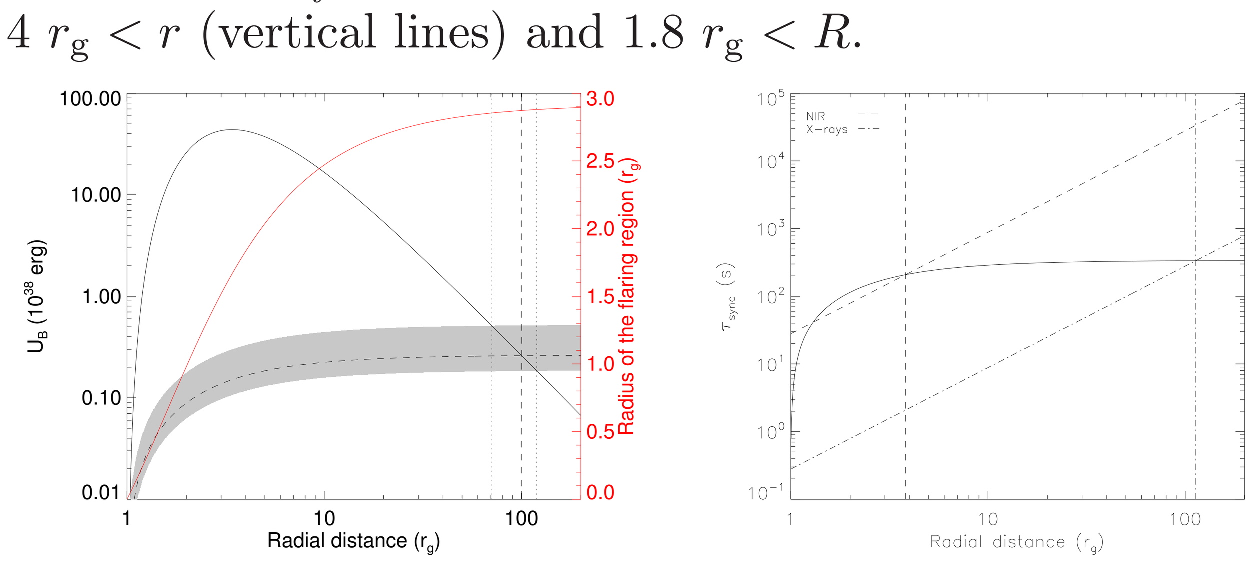

Figure 4: Constraints on the radial distance and the radius of the flaring region. *Left panel:* The black and red lines are the distribution of the magnetic energy and the source radius, respectively. The dashed line and the gray stripe are the X-ray fluence and the error bars. *Right panel:* The synchrotron cooling during the decay phase.

Conclusion

- Two X-ray flares are detected during the 2011 XMM-Newton campaign with the Bayesian-blocks analysis.
- We developed a hotspot model to explain the double-peak shape of the 2011 March 30 flare. However, the decrease of the flux back to the quiescent level between the two substructures cannot be satisfactorily reproduced without adding some ad hoc components.
- The very rapid flux variation during the first sub-flare allow us to constrain the distance and the size of the flaring source. Computing the proper time around a supermassive black hole and fixing $B \propto r^{-1}$ with $B = 100$ G at $2\,r_{\rm g}$ and assuming that the rise and decay phases are due to magnetic energy heating and synchrotron cooling of infrared photons, respectively, we derive a range to the radial distance of $4 - 100^{+19}_{-29}\ {\rm r_g}$. The corresponding source radii at this distance are $1.8 - 2.87 \pm 0.01\ {\rm r_g}$